Mechanism and Machine Theory 71 (2014) 126–141

Contents lists available at ScienceDirect

Mechanism and Machine Theory

journal homepage: www.elsevier.com/locate/mechmt

Design theory and dynamic analysis of a deployable boom

ZhongYi Chu *, YiAn Lei

Science and Technology on Inertial Laboratory, Beihang University, XueYuan Road, 100191 Beijing, China

ARTICLE INFO

Article history:
Received 12 November 2012
Received in revised form 18 June 2013
Accepted 21 September 2013
Available online 17 October 2013

Keywords:
Deployable boom
Dynamic analysis
Optimal design
Finite element method

ABSTRACT

The deployable boom plays an important role in the realisation of various spacecraft missions. In this paper, we will propose a deployable boom that is composed of a lenticular boom with a storage reel, a retractable/deployable mechanism and other auxiliary devices for use in a small spacecraft. To satisfy the requirements of specific specifications, such as having a small stowed volume, being light weight, having a large magnification ratio and an unrumpled retraction/deployment, an optimal design of the deployable boom is developed based on a review of its mechanical analysis. Therefore, the parameters of the boom's cross-section and the diameter of the storage reel are optimised using definite geometrical and physical constrains. Furthermore, by considering the geometrical dimensions and the energy equilibrium relationship constrains, key parameters of the retractable/deployable mechanism are deduced. Additionally, it is valuable to mention that the sequential quadratic programming method is adopted to reduce the computational complexity. Finally, the results of a finite element method are in good agreement with the aforementioned theoretical prediction, which validates the efficiency of the optimal design for the deployable boom.

1. Introduction

Various spacecraft missions have resulted in the need for larger, stronger and lighter deployable structures, which help to hold instruments, such as magnetometers, away from the spacecraft to avoid a disturbance caused by remanence of the spacecraft body (see Fig. 1(a)). These deployable structures are usually stowed in a compact volume in the launch vehicle and are deployed to large surfaces or large volumes in space. In general, the deployable structures can be classified into hinged, linear, surface and volume deployable structures. Among these groups, the linear deployable booms, with subtypes such as telescoping, inflatable, articulated or coiled and tubular extendable booms, are the simplest and most frequently used. Since the deployable boom was first proposed by the National Aeronautics and Space Administration (NASA), different deployable booms have been developed. As shown in Fig. 1(b)(1)(2), the tubular extendable booms (including the STEM and BI-STEM) are the most popular and have been commercially available for decades. However, the open cross-section geometry makes these booms prone to bucking under non-axial loading. To overcome this buckling problem, a cross-section geometry can be used to increase the stiffness of the boom, such as the lenticular boom (see Figs. 1(b)(3)). NASA proposed an 18-metre-long lenticular deployable boom for the space shuttle [1] and an instrument deployable mechanism for the THEMIS satellite [2]. The German Aerospace Centre (DLR) also developed a $20 \times 20\ m^2$ solar-sail deployable mechanism that includes four high-performance and large carbon fibre reinforced plastic (CFRP) lenticular booms. This mechanism was studied in weightlessness, and very satisfactory results were obtained [3–7]. Roybal made a triangular retractable and collapsible (TRAC) deployable boom, which has a triangular cross section and better performance [8,9]. Recently, NASA designed an advanced collapsible rollable tube (CRT) mechanism for reconfigurable small spacecraft [10].

Although the aforementioned deployable booms have different styles and structures, they are all based on careful design. In the process of designing the deployable boom, geometrical limitations and mechanical performances imposed by the design

* Corresponding author at: Beihang University, Xue Yuan Road, Beijing, China. Tel.: +86 13552712797.
E-mail address: chuzy@buaa.edu.cn (Z. Chu).

0094-114X/$ – see front matter © 2013 Elsevier Ltd. All rights reserved.
http://dx.doi.org/10.1016/j.mechmachtheory.2013.09.009

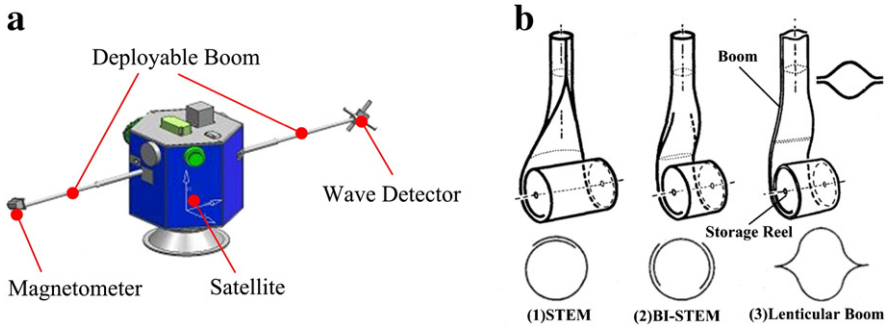

Fig. 1. (a) Application of deployable boom. (b) Different tubular extendable booms.

requirements, such as stowed and deployed volume, intensity, bending and torsional stiffness, natural frequency, energy equilibrium of the retractable/deployable process, etc., must first be met. Many studies of the mechanical performance of the deployable boom have been reported. Hakkak proposed simple formulas and models to provide good initial plans for a lenticular boom, which were perfectly adequate for the primary design [11]. Pellegrino studied the shell structures theory in the past decades, and very remarkable works have been made. He built a comprehensive analytical model of the bistable cylindrical shells to predict the residual stress distribution, which was in good agreement with experimental results [12,13]. And he also studied the folding and deployment behaviours of the curved tape springs, which have significant value to the proper design of the deployable booms [14]. Rehnamark gave a detailed introduction of a lenticular boom and an energy analysis of the deployment mechanism [10], which was tested in a terrestrial environment, and satisfactory results were obtained [15]. Although significant efforts have been made to analyse the mechanical performance of the deployable boom, researchers are urgently pursuing an efficient design solution for the deployable boom that should satisfy the requirements of special tasks.

However, computational complexity usually exists in the optimal design of the deployable boom. Li studied the stowing and deploying performance of a CFRP lenticular boom using an accurate finite element method (FEM) model, but a single simulation of the accurate FEM model would take more than twenty hours [16,17]. Classical optimisation methods are very efficient and easy to implement [18,19], but these methods cannot change the topological structure during calculation and are not suitable for nonlinear problems, which narrow the constraint scope. Therefore, a more efficient optimal solution especially for nonlinear optimisation problems is the correct choice for the design of a deployable boom.

This paper presents the optimal design and a dynamic analysis of a deployable boom. Firstly, the mechanical analysis is implemented to investigate the characteristics of the deployable boom. Then, to achieve the goal of minimising the maximum stress in the boom, the parameters of the boom cross-section and the diameter of the storage reel are optimised. Furthermore, to minimise the mass of the spring and the power of the motor, the optimal design of the retractable/deployable mechanism is developed. It is valuable to mention that the SQP is also adopted to reduce the computational complexity of the optimisation. Finally, to validate the efficiency of the design, FEM is applied to investigate the mechanical behaviours of the deployable boom, which are in good agreement with theoretical prediction. The novelty of this work is to design a deployable boom of micro satellite for a space probe, which is driven by motor cooperated with reactive springs to satisfy the specifications of small stowed volume, large magnification ratio and energy saving. In addition, it is valuable to note that the optimization and dynamical behaviours of the proposed boom are detailed investigated in this paper.

This paper consists of six sections, and the rest of the paper is organised as follows. In Section 2, the conceptual design of the deployable boom is introduced. Based on the mechanical analysis of the deployable boom in Section 3, the detailed optimal design of the deployable boom is proposed in Section 4. Then, the corresponding FEM model and analysis results of the designed boom are discussed in Section 5. Finally, the conclusions are given in Section 6.

2. Brief overview of the deployable boom

2.1. Structure and operating principle

As shown in Fig. 2, the proposed deployable boom consists of three parts: (1) the lenticular boom with a storage reel; (2) the retractable/ deployable mechanism; and (3) other auxiliary devices. The lenticular boom is assembled from two omega-shaped half-shells that are made from carbon fibre reinforced plastic (CFRP) materials (parameters of the material are shown in Table 1). The shells' cross-sections are hollow, lenticular, thin-walled and symmetric; thus, it is very convenient to use a storage reel to save space when stowing the boom. The storage reel consists of an aluminium reel in which the support bearings and the reaction springs are embedded. The retractable/deployable mechanism consists of a drive motor, an active roller, a negative roller, a roller chain, a guide plate and two swing arms. When the boom is deploying, the drive motor provides the positive moment, the guide plate protects the boom from physical damage, and the swing arms help to support the negative roller, which cooperates with the active roller to ensure unrumple in flattening the boom. Other auxiliary devices include three support beams, a support collar and

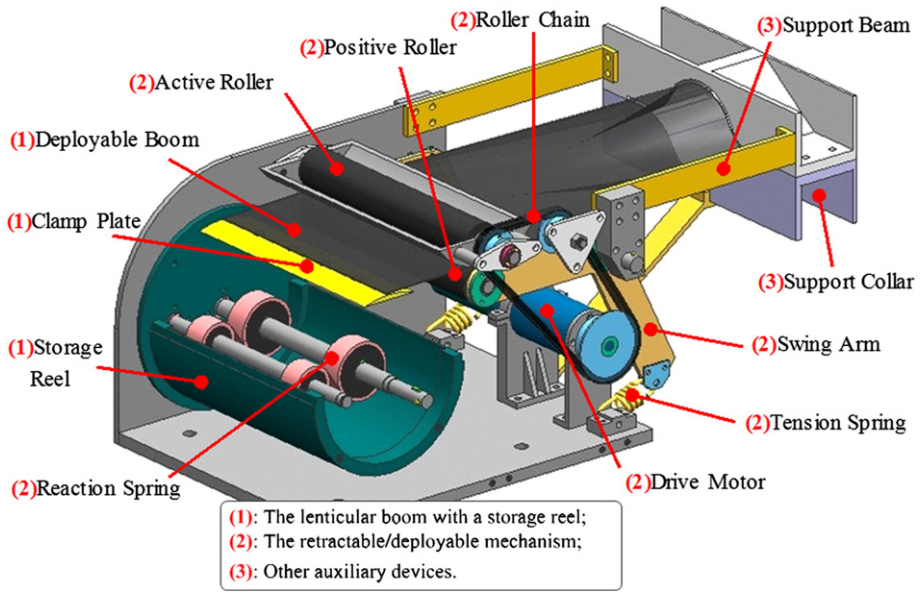

Fig. 2. Structure of the deployable boom.

other support devices are used to maintain the relative positions of the subsystems. Specifically, the active roller and the support collar provide boundary conditions for the boom transition region. The three parts work together to constitute the integrated deployable boom.

The operating principle of the deployable boom can be divided into two types: deploying and retracting. When in deploying mode, the motor drives the active roller by means of a roller chain and guides the flattened boom that is unrumpled when deploying. Simultaneously, the reaction springs will store potential energy to provide a reasonable reverse moment, and the deployed boom changes its flattened cross-section shape to its primary state. When in retracting mode, the drive motor changes its direction and drives the active roller to flatten the boom. The reaction springs provide an approximately constant moment by releasing energy to help wrap the boom without rumpled. The boom will change its cross-section shape from a curved to a flattened state.

2.2. Specification requirements

Considering the requirements of both the deployable boom design and the small spacecraft demand, the specifications of the deployable boom are presented as follows.

(1) Mass of the payload on the tip of the boom: more than 0.7 kg.
(2) Deployed length of the boom: at least 1.5 m.
(3) Stowed volume of the entire system: no more than $320 \times 160 \times 120$ mm^3.
(4) Frequency in the deploying process: greater than 5 Hz.
(5) Time of the deploying process: no more than 60 s.
(6) Material of the boom requirement: nonmagnetic, flexibility (stowed state) and rigidity (deployed state).

Table 1
Material characteristics of the boom and spring.

Parameter	Symbol	Value
Young's modulus of the boom	E	110 GPa
Poisson's ratio of the boom	μ	0.3
Density of the boom	ρ	1600 kg/m^3
Young's modulus of the spring	E_1	193 GPa
Poisson's ratio of the spring	μ_1	0.3
Density of the spring	ρ_1	7800 kg/m^3
Allowable normal stress	$[\sigma]$	1570 MPa
Allowable shear stress	$[\tau]$	1570 MPa

3. Mechanical analysis

The mechanical analysis of the *deployable boom* is the foundation of the design, especially with respect to the performances of some key components. Therefore, the material property and geometrical dimension of the *lenticular boom and the storage reel* determine the maximum stress, the carrying capacity and the natural frequency. The structure of the *reaction spring* determines the torsional moment and the mass of the spring. Conversely, the energy equilibrium relationship of the entire system determines the minimum moment and the revolutions of the *motor* and ensures unrumpled retraction/deployment of the lenticular boom. Therefore, it is necessary to analyse the mechanical characteristics of the lenticular boom in detail before the optimal design.

3.1. Static analysis

3.1.1. Bending stress of the lenticular boom

When the lenticular boom with a tip mass is deployed, it is equivalent to a cantilever beam-mass model. As shown in Fig. 3, the cross-section of the lenticular boom is symmetric, so it is sufficient to calculate the bending stiffness by multiplying the result of a quarter of the section by four.

The moment of area about the x-axis, I_x, and the maximum bending stress, σ_{b_x}, can be calculated as [11]

$$I_x = 4\int_0^{x_1} tr_1 \frac{\left(\sqrt{r_1^2\text{-}x^2} + y_{0,1}\right)^2}{\sqrt{r_1^2\text{-}x^2}}dx + 4\int_{x_1}^{x_2} tr_2 \frac{\left[-\sqrt{r_2^2\text{-}(x\text{-}x_2)^2} + y_{0,2}\right]^2}{\sqrt{r_2^2\text{-}(x\text{-}x_2)^2}}dx \tag{1}$$

$$\sigma_{b\_x} = \frac{\left(mgl + 0.5ql^2\right)\left(r_1 + y_{0,1}\right)}{I_x}. \tag{2}$$

The moment of area about the y-axis, I_y, and the maximum bending stress, σ_{b_y}, can be obtained using a similar method

$$I_y = 4\int_0^{x_1} tr_1 \frac{x^2}{\sqrt{r_1^2\text{-}x^2}}dx + 4\int_{x_1}^{x_2} tr_2 \frac{x^2}{\sqrt{r_2^2\text{-}(x\text{-}x_2)^2}}dx + 4\int_{x_2}^{x_3} tx^2 dx \tag{3}$$

$$\sigma_{b\_y} = \frac{\left(mgl + 0.5ql^2\right)x_3}{I_y}, \tag{4}$$

where t is the thickness of the section; r_1 and r_2 are the radii of the left and right circular arcs, respectively; $x_{0,1}$, $y_{0,1}$, $x_{0,2}$ and $y_{0,2}$ correspond to the x- and y-coordinates of the left and right circular centre, respectively; m is the mass of the tip load; g is the acceleration due to gravity; l is length of the deployed boom; and q is the linear distributed load of the boom along the deployed direction.

Therefore, the maximum bending stress in the boom, σ_{b_max}, can be expressed as

$$\sigma_{b\_max} = max\left(\sigma_{b_x}, \sigma_{b_y}\right). \tag{5}$$

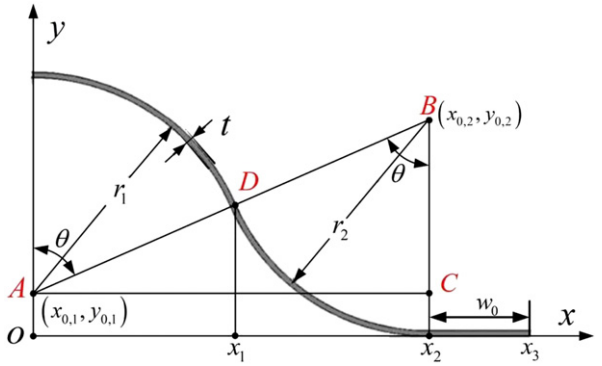

Fig. 3. Cross-section for a quarter of the lenticular boom.

3.1.2. Torsional stress of the lenticular boom

As the lenticular boom is a thin-walled, hollow tube (see Fig. 3), the equivalent torsional moment of area, J_t, and the maximum shear stress of the boom, τ_t, can be written as [11]

$$J_t = \frac{4A^2}{\oint \frac{dP}{t}} = \frac{16t\left\{\int_0^{x_1}\left(\sqrt{r_1^2\text{-}x^2}+y_{0,1}\right)dx + \int_{x_1}^{x_2}\left(-\sqrt{r_2^2\text{-}(x\text{-}x_2)^2}+y_{0,2}\right)dx\right\}^2}{\int_0^{x_1} r_1/\sqrt{r_1^2\text{-}x^2}dx + \int_{x_1}^{x_2} r_2/\sqrt{r_2^2\text{-}(x\text{-}x_2)^2}dx} \tag{6}$$

$$\tau_t = \frac{T}{2At}, \tag{7}$$

where A is the cross-sectional area of the boom (neglecting the straight part of the section), P is the perimeter of the area and T is the torsional moment.

3.1.3. Geometrical relationship of the boom cross-section

In Fig. 3, when the boom is flattened, the width of the boom can be written as

$$w = 2[w_0 + (r_1 + r_2)\theta], \tag{8}$$

where w_0 is the width of the straight part of the boom cross-section and θ is the central angle of the two arcs.

As shown in Fig. 3, the other geometrical relationship in triangle ABC can be determined as

$$\cos\theta = \frac{r_2\text{-}y_{0,1}}{r_1 + r_2}, \tag{9}$$

where $y_{0,1}$ is the y-coordinate of the left circular centre.

Combining Eqs. (8) and (9), we can obtain

$$w = 2\left[w_0 + (r_1 + r_2)\arccos\left(\frac{r_2\text{-}y_{0,1}}{r_1 + r_2}\right)\right]. \tag{10}$$

3.1.4. Maximum flattened and wrapped stress in the lenticular boom

As shown in Fig. 4(a), the boom is flattened and wrapped separately. As shown in Fig. 3, the radii of the circular arcs (r_1, r_2) are much larger than the thickness of the boom shell, t; thus, the maximum flattened normal stress in the boom, σ_{s_x}, can be written as

$$\sigma_{s\_x} = \frac{Et}{2r_{\min}}, \tag{11}$$

where

$$r_{min} = min(r_1, r_2).$$

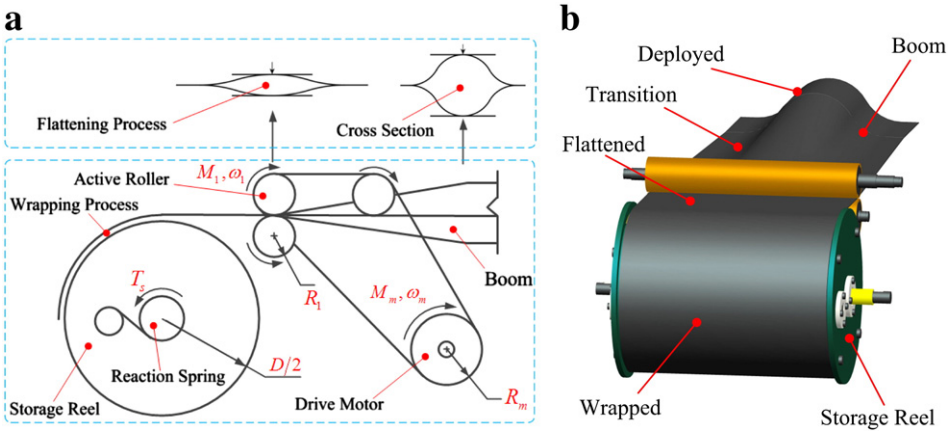

Fig. 4. (a) Flattening and wrapping process of the lenticular boom. (b) Side view of the wrapped lenticular boom.

The flattened boom will be wrapped around a storage reel (whose diameter is D). When boom is wrapped, the thickness of two attached boom shell (straight part) should be 2 t, thus the maximum wrapping normal stress will be

$$\sigma_{s\_y} = \frac{2Et}{D}. \tag{12}$$

Then, Mohr's circle of stresses will be applied to find the maximum stowed normal and shear stresses [11]:

$$\sigma_{s\_max} = max\left(\sigma_{s\_x}, \sigma_{s\_y}\right) = max\left(\frac{Et}{2r_{min}}, \frac{2Et}{D}\right) \tag{13}$$

$$\tau_{s\_max} = \frac{1}{2}\left(\sigma_{s\_x} + \sigma_{s\_y}\right) = \frac{1}{2}\left(\frac{Et}{2r_{min}} + \frac{2Et}{D}\right). \tag{14}$$

Therefore, combining Eqs. (5) and (14), the maximum normal stress in the lenticular boom, σ_{max}, can be written as

$$\sigma_{max} = max\left(\sigma_{b\_max}, \sigma_{s\_max}\right). \tag{15}$$

3.2. Dynamic analysis

3.2.1. Natural frequency

When the lenticular boom is deployed, the vibration problem must be taken into consideration to reduce the influence on the spacecraft. To understand the vibration properties of the boom, the natural frequencies are calculated. Here, an approximate equation is used to determine the first and second order natural frequencies as [20]

$$\lambda = \frac{1}{2\pi}\sqrt{\frac{3EI}{ml^3 + 0.236ql^4/g}}, \tag{16}$$

where E is the Young's modulus, I is the moment of inertia and l is the deployed length of the boom.

3.2.2. Strain energy of the reaction spring

The geometry of one reaction spring is shown in Fig. 5, and the torsional moment can be written as [10]

$$T_s = \frac{E_1 b_1 D_2 t_1^3}{12(1\text{-}\mu_1^2)}\left(\frac{1}{D_1} + \frac{1}{D_2}\right)^2, \tag{17}$$

where E_1, b_1, t_1 and μ_1 correspond to the elastic modulus, the width, the thickness and the Poisson's ratio of the spring tape material, respectively; D_1 and d_1 are the outer and inner diameters of the storage drum; and D_2 and d_2 are the outer and inner diameters of the output drum.

Two power springs are embedded in the storage reel and used for storing/releasing energy. D_1 and D_2 in Eq. (17) are variable as the reaction spring rotates, so the strain energy of one reaction spring can be approximated by

$$U_s = \int_0^{\theta_f} T_s d\theta \approx T_{s1}\frac{L}{D/2}, \tag{18}$$

where θ is the rotational angel of the spring, D is the diameter of the storage reel, T_{s1} is the average torsional moment of the reaction spring, and L is the total length of the deployed boom.

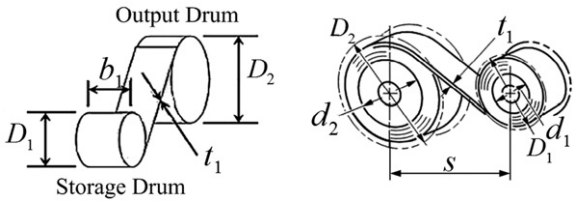

Fig. 5. Geometry of the reaction spring.

When the boom is deploying, the spring moves from the storage drum to the output drum, so some important relationships below must be tenable:

$$\frac{\pi}{4}\left(D_{2,\max}^2-d_2^2\right)=\frac{\pi}{4}\left(D_{1,\max}^2-d_1^2\right)=kL_st_1 \tag{19}$$

$$X_s=s+D_{1,\max}/2 \tag{20}$$

$$L_{eq}=\frac{L}{(D/2)}\cdot\frac{D_{2,\max}}{2}=\frac{D_{2,\max}L}{D} \tag{21}$$

$$m_s=\left[2L_st_1b_1+\frac{\pi}{4}b_1\left(d_1^2+d_2^2\right)\right]\rho, \tag{22}$$

where $D_{2,max}$ is the outer diameter of the output drum when the spring is fully stowed on the drum, $D_{1,max}$ is the outer diameter of the storage drum when spring is fully stowed on the drum, k is the constant coefficient and is equal to 1.25, L_s is the total length of the tape spring, X_s is the maximum geometrical length of the spring, s is the distance between the two drums' centre (usually $s = D_{2,max}$), L_{eq} is equal to the length of deployed boom, m_s is the mass of one reaction spring, and ρ is the density of the spring material.

3.2.3. Strain energy in the lenticular boom

The strain energy stored in the retracted boom consists of the flattened strain energy and the wrapped counterpart. To obtain an approximate estimation of the value, the top and bottom half of the boom can be modelled as separate thin-walled elastic shells with isotropic material properties [14].

The flattened strain energy in the boom, U_{bf}, can be estimated as

$$U_{bf}=2U_{bf\text{-}half}=2\int_0^W\frac{M_z^2}{2E'I_z}dw=E'I_z\left(\frac{w_1}{r_1^2}+2\frac{w_2}{r_2^2}\right), \tag{23}$$

where M_z is the moment of the beam along the z-axis, E' is equal to $E/(1\text{-}\mu^2)$ according to the generalised Hook's law, E is the Young's modulus of the material, μ is the Poisson's ratio, I_z is the moment of inertia of the boom along the z-axis and can be approximated by $Lt^3/12$, L is the total length of the deployed boom, t is the thickness of the boom shell, w_1 and w_2 are the lengths of the circular arcs, and r_1 and r_2 are the radii of the circular arcs (see Fig. 3).

After being flattened, the lenticular boom will be wrapped on the storage reel. The wrapped strain energy, U_{bw}, can be written as

$$U_{bw}=2U_{bw\text{-}half}=2\int_0^L\frac{M_x^2}{2E'I_x}dl=\frac{E'I_xL}{(D/2)^2}, \tag{24}$$

where M_x is the moment of the beam along x-axis, I_x is the moment of inertia of the boom along the z-axis and can be approximated by $wt^3/12$, D is the diameter of the storage reel, and w is the width of the flattened boom and equal to $w_0 + w_1 + w_2$.

The total strain energy of the lenticular boom is the sum of the flattened and wrapped strain energies

$$U_b=U_{bf}+U_{bw}\ . \tag{25}$$

3.2.4. Energy provided by the drive motor

Generally, the energy provided by the motor can be expressed as

$$U_m=P_mt_d, \tag{26}$$

where P_m is the power provided by the motor and t_d is the required time to finish deploying or retracting the boom.

As shown in Fig. 4(a), P_m and t_d can be further written as

$$t_d=\frac{L}{\omega_1R_1},\quad P_m=M_m\omega_m,\quad \omega_mR_m=\omega_1R_1, \tag{27}$$

where ω_1 is the angular velocity of the active roller, R_1 is the radius of the active roller, M_m is the torsional moment of the drive motor, ω_m is the rated speed of the drive motor, and R_m is the radius of the output drum of the motor.

Combining Eqs. (26) and (27), we can obtain

$$U_m=\frac{M_m}{R_m}L\ . \tag{28}$$

4. Optimal design of the deployable boom

Based on the mechanical analysis and considering some geometrical dimensions and physical constraints, two optimal models of the lenticular boom with the storage reel and the retractable/deployable mechanism are built to optimise the design variables of the lenticular boom. Furthermore, considering the balance between accuracy and efficiency, we solve the two optimisation models using the sequential quadratic programming (SQP) method [21].

4.1. Optimisation model

4.1.1. Optimisation model of the lenticular boom with the storage reel

According to the analysis above, the specifications of the lenticular boom, including the width of the flattened boom (w), the maximum normal stress in boom (σ_{max}), the maximum shear stress in boom (τ_{max}), and the first-order natural frequency (λ), have a great influence on the deployable boom system. To improve the optimisation efficiency, these items are selected as constraint variables and are expressed in a vector as

$$\mathrm{D}_1 = [w \;\; \sigma_{max} \;\; \tau_{max} \;\; \lambda]^T. \tag{29}$$

Based on the analysis in Eqs. (10), (14), (15) and (16), the expressions in Eq. (29) are determined by the circular radii (r_1 and r_2), the y-coordinate of the circular centre ($y_{0,1}$), the width of the flattened boom (w_0), the diameter of the storage reel (D), the thickness of the boom shell (t) and the total length of the deployed boom (L). Thus, the optimal design variables can be written in a vector as

$$\mathrm{X}_1 = \left[r_1 \; r_2 \; y_{0,1} \;\; w_0 \;\; D \quad t \quad L\right]^T. \tag{30}$$

According to the structure of the lenticular boom and engineering experience, the geometrical dimension constrains of design variables can be defined as

$$\begin{cases} 2\ \text{cm} \le r_1 \le 3\ \text{cm} \\ 2\ \text{cm} \le r_2 \le 3\ \text{cm} \\ 0 \le y_{0,1} \le 1.5\ \text{cm} \\ 1\ \text{cm} \le w_0 \le 2\ \text{cm} \\ 7\ \text{cm} \le D \le 9\ \text{cm} \\ 0.25\ \text{mm} \le t \le 0.35\ \text{mm} \\ 1.5\ \text{m} \le L \le 2\ \text{m} \end{cases}. \tag{31}$$

Conversely, the physical constraint conditions are arranged as follows. Firstly, according to the requirement of the stowed volume of the entire system, the width of the flattened boom, w, should be less than 12 cm. Then, to ensure the safety of the boom, the maximum normal and shear stresses in the stowed boom, σ_{max} and τ_{max}, should be less than half of the allowable stress, $[\sigma]$ and $[\tau]$. Finally, the first-order natural frequency, λ, should be greater than the limitation. Therefore, the physical constraint conditions should be written as

$$\begin{cases} \sigma_{max} \le 785\ \text{MPa} \\ \tau_{max} \le 785\ \text{MPa} \\ w \le 12\ \text{cm} \\ \lambda \ge 5\ \text{Hz} \end{cases}. \tag{32}$$

As the boom is made of a CFRP material, which is very light, and the mass requirement can be easily satisfied. A small stress in the boom results in a safer lenticular boom. Therefore, the objective of the optimal design is to minimise the stress in the boom under the constraints mentioned above. Because the constraint conditions are nonlinear, the optimisation becomes a nonlinear problem with multiple design variables, and the objective function can be written as

$$M_1 = p_1\sigma_{max} + p_2\tau_{max} = min \;\; f_1\left(r_1, r_2, y_{0,1}, w_0, D, t, L\right), \tag{33}$$

where p_1 and p_2 are the weight factors.

4.1.2. Optimisation model of the retractable/deployable mechanism

The structure of the retractable/deployable mechanism is shown in Fig. 4, and the challenge is to design a cabinet reaction spring to fit inside the storage reel while providing sufficient torque to keep the boom wound around the storage reel actively when the boom is retracting. For the energy equilibrium relationship, it is an essential demand to ensure an unrumpled retraction/deployment of the deployable boom. According to the analysis above, the specifications of the retractable/deployable mechanism include the maximum geometrical length of the reaction spring, X_s; the length of the spring tape, L_s; the energy of the

spring, U_s; the energy of the motor, U_m; and the deployed time, t_d. These parameters are selected as constraint variables, which can be expressed in vector form as

$$\mathrm{D}_2 = [X_s \quad L_s \quad U_s \quad U_m \; t_d]^T. \tag{34}$$

Based on the analysis in Eqs. (18), (19), (20), (27) and (28), the expressions in Eq. (34) are determined by the inner diameters of the spring storage drum and output drum, d_1 and d_2; the length of the spring tape, L_s; the thickness and width of the reaction spring, t_1 and b_1; and the moment, the output drum radius and the revolutions of the drive motor, M_m, R_m and ω_m, respectively. So the optimal design variables can be written in vector form as

$$\mathrm{X}_2 = [d_1 \quad d_2 \quad L_s \quad t_1 \quad b_1 \quad M_m \quad R_m \quad \omega_m]^T. \tag{35}$$

According to the structure of the deployable mechanism and engineering experience, the geometrical dimension constrains of the design variables should be defined as

$$\begin{cases} 14\ \mathrm{mm} \le d_1 \le 20\ \mathrm{mm} \\ 24\ \mathrm{mm} \le d_2 \le 30\ \mathrm{mm} \\ 55\ \mathrm{cm} \le L_s \le 80\ \mathrm{cm} \\ 0.2\ \mathrm{mm} \le t_1 \le 0.3\ \mathrm{mm} \\ 10\ \mathrm{mm} \le b_1 \le 16\ \mathrm{mm} \\ 1\ \mathrm{Nm} \le M_m \le 3\ \mathrm{Nm} \\ 30\ \mathrm{mm} \le R_m \le 40\ \mathrm{mm} \\ 10\ \mathrm{r/min} \le \omega_m \le 30\ \mathrm{r/min} \end{cases}. \tag{36}$$

Additionally, the physical constraint conditions are prescribed as follows. Firstly, according to the volume of the storage reel, the maximum geometrical length of the spring (see Eq. (20)), X_s, should be less than half of the diameter of the storage reel. Secondly, the length of the tape spring (see Eq. (19)), L_s, must be longer than the length of the deployed boom (see Eq. (21)), L_{eq}. Furthermore, the energy equilibrium relationship is taken into consideration. In the deploying process, the drive motor provides power for the system, the lenticular boom releases wrapping strain energy and the reaction springs store potential energy; thus, the energy provided by the motor, U_m, must be greater than the energy of the reaction springs, U_s, to ensure the proper function of the system. In the retracting process, the drive motor does the work of flattening the boom, so the energy of motor, U_m, should be greater than the boom flattening energy, U_{bf}. The reaction springs are responsible for wrapping the boom, so the energy of the reaction springs, U_s, should be greater than the boom wrapping energy, U_{bw}. The relationship between the net spooling energy, U_n (the net spooling energy is equal to the boom wrapping energy plus the reaction spring energy), and the deployed length, l, should satisfy some requirements. Along with the boom deploying, the slope of the "Net Spooling Energy" must be positive. The deployed boom represents a higher energy state for the system than the stowed boom, and work is performed by the drive motor to extend the boom. Therefore, the boom can stay tightly wrapped around the storage reel when the system is in its lowest energy state [10]. Additionally, considering the requirement of the deployable task, the time is limited to 60 s.

According to the upper analysis, the physical constraint conditions should be written as

$$\begin{cases} X_s < D/2 \\ L_s > L_{eq} \\ U_m > U_{bf} \\ U_{bw} < U_s < U_m \\ t_d < 60s \end{cases}. \tag{37}$$

It is valuable to mention that the reaction spring is made up of 301 stainless steel and the spring drums are made up of Q235 steel; therefore, the mass requirement should be taken into consideration. Conversely, the power consumption of the motor is limited by the satellite requirement. Therefore, the optimal design of the retractable/deployable mechanism is minimising the mass of the reaction spring, m_s, and the power of the motor under the constraints mentioned above. As the constraints are nonlinear, the optimisation becomes a nonlinear problem with multiple design variables, and the objective function can be written as

$$M_2 = q_1 m_s + q_2 P_m = min \; f_2(d_1, d_2, L_s, t_1, b_1, M_m, R_m, \omega_m). \tag{38}$$

where q_1 and q_2 are the weight factors.

4.2. Optimisation method and results

The SQP method is used to search for the optimal solutions of the deployable boom with the storage reel and the retractable/deployable mechanism. The detailed flow chart for the optimal design can be shown in Fig. 6.

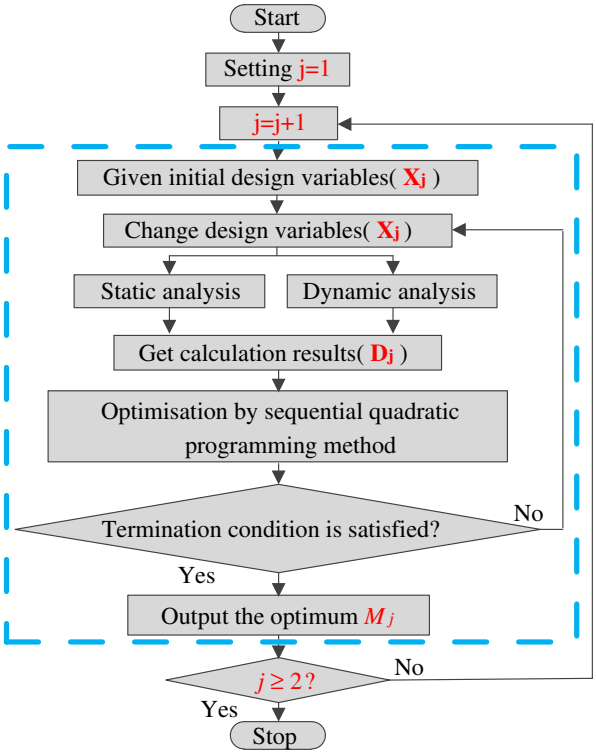

Fig. 6. Flow chart for the optimisation programme.

Considering the conditions of design variables and other subjective factors, the initial design variables can be selected as

$$\begin{aligned} X_{1,0} &= \left[r_1\, r_2\, y_{0,1}\, w_0\, D \quad t \quad L\right]^T \\ &= [3\ \text{cm}\ \ 2\ \text{cm}\ \ 1\ \text{cm}\ \ 1.5\ \text{cm}\ \ 8\ \text{cm}\ \ 0.3\ \text{mm}\ \ 2\ \text{m}]^T \end{aligned} \tag{39}$$

$$\begin{aligned} X_{2,0} &= [d_1 \quad d_2 \quad L_s \quad t_1 \quad b_1 \quad M_m \quad R_m \quad \omega_n]^T \\ &= [18\ \text{mm}\ \ 28\ \text{mm}\ \ 70\ \text{cm}\ \ 0.25\ \text{mm}\ \ 14\ \text{mm}\ \ 2\ \text{Nm}\ \ 35\ \text{mm}\ \ 25\ \text{r/min}]^T\ . \end{aligned} \tag{40}$$

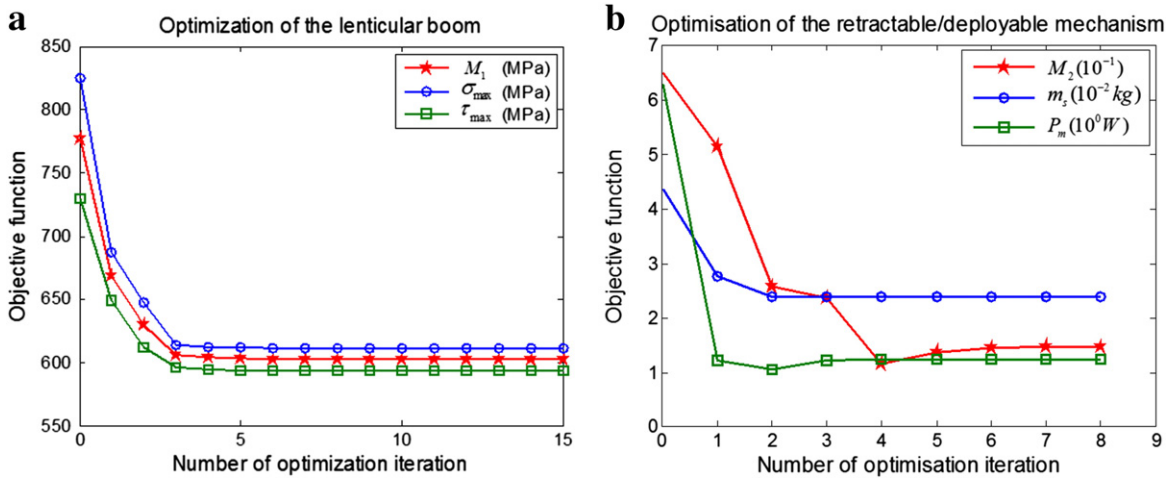

Fig. 7. (a) Optimisation of the lenticular boom with the storage reel. (b) Optimisation of the retractable/deployable mechanism.

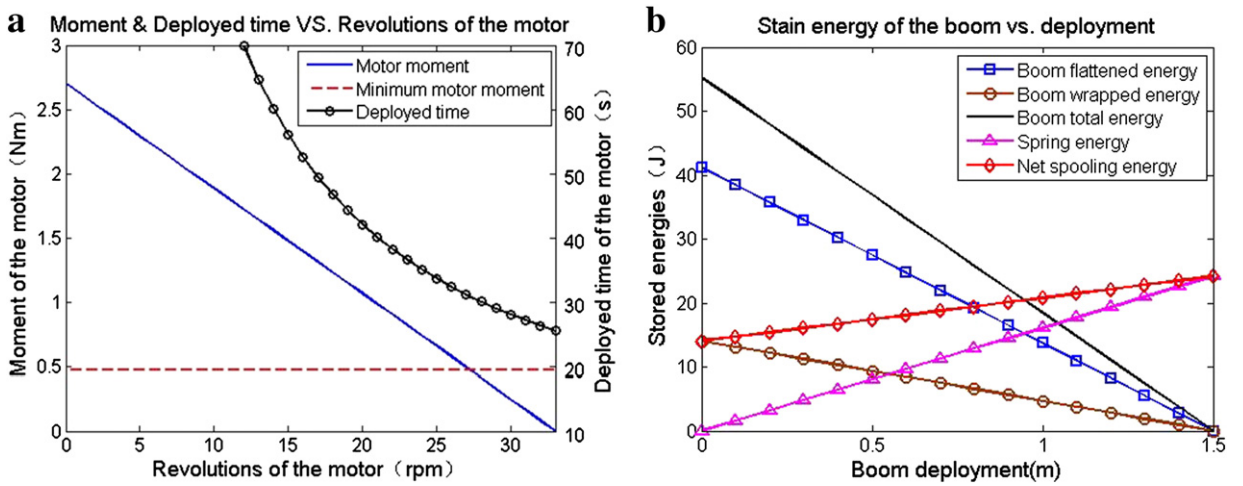

Fig. 8. (a) Moment and deployed time versus revolutions of the motor. (b) Strain energy of the deployable boom system.

The weight factors of the objective functions (Eqs. (33) and (38)) are selected as

$$p_1 = 0.5,\ \ p_2 = 0.5,\ \ q_1 = 0.9,\ \ q_2 = 0.1. \tag{41}$$

As shown in Fig. 6, the terminal condition of the SQP method is selected to be 0.001 considering both the efficiency and the accuracy.

The optimal problem can be easily solved using the SQP toolbox in Matlab software [22]. The optimal results of the objective functions in Eqs. (33) and (38) are shown in Fig. 7. The normal/shear stress in the boom and the mass of the reaction spring as well as the power of the motor reach a minimum after ten iterations.

The corresponding values of the constraint variables satisfy the requirements of physical practicality:

$$\mathrm{D}_{1,final} = [w \quad \sigma_{max} \ \ \tau_{max} \ \ \lambda]^T = [12\ \text{cm}\ \ 611\ \text{MPa}\ \ 593\ \text{MPa}\ \ 6.12\ \text{Hz}]^T, \tag{42}$$

$$\mathrm{D}_{2,final} = [X_s \quad L_s \quad U_s \quad U_m \quad t_d]^T = [4.02\ \text{cm}\ \ 61.5\ \text{cm}\ \ 25.13\ \text{J}\ \ 75\ \text{J}\ \ 60\ \text{s}]^T. \tag{43}$$

The optimal results of the design variables can also be obtained:

$$\begin{aligned} \mathrm{X}_{1,final} &= \left[r_1 \ \ r_2 \ \ y_{0,1} \ \ w_0 \ \ D \quad t \quad L\right]^T \\ &= [2.4\ \text{cm}\ \ 2.4\ \text{cm}\ \ 0\ \text{cm}\ \ 1\ \text{cm}\ \ 9\ \text{cm}\ \ 0.3\ \text{mm}\ \ 1.69\ \text{m}]^T, \end{aligned} \tag{44}$$

$$\begin{aligned} \mathrm{X}_{2,final} &= [d_1 \ \ d_2 \ \ L_s \ \ t_1 \ \ b_1 \ \ M_m \ \ R_m \ \ \omega_n]^T \\ &= [16\ \text{mm}\ \ 26\ \text{mm}\ \ 61.5\ \text{cm}\ \ 0.2\ \text{mm}\ \ 12.4\ \text{mm}\ \ 1\ \text{Nm}\ \ 20\ \text{mm}\ \ 12\ \text{r/min}]^T. \end{aligned} \tag{45}$$

However, considering other factors in application, for example, as the ideal moment has a linear relationship with the revolutions of the selected motor, a plot is needed to determine the moment of the motor (see Fig. 8(a)). Based on the deployed time requirement and the minimum moment in the plot, we can determine the revolutions of the drive motor as 15 r/min and the moment of the motor as 1.5 Nm. Lastly, the values of the designed variables are chosen as shown in Tables 2 and 3. The strain energy versus the deployed boom length is shown in Fig. 8(b). From the plot, we can see that the net spooling energy has a

Table 2
Designed values of the lenticular boom with the storage reel.

Parameter	Symbol	Value
Radius of the left circular arc	r_1	2.4 cm
Radius of the right circular arc	r_2	2.4 cm
Y-coordinate of the left circular centre	$y_{0.1}$	0 cm
Width of the straight part	w_0	1.0 cm
Diameter of the storage reel	D	9 cm
Thickness of the boom shell	t	0.25 mm
Total length of the boom	L	1.5 m

Table 3
Designed values of the retractable/deployable mechanism.

Parameter	Symbol	Value
Inner diameter of the storage drum	d_1	16 mm
Inner diameter of the output drum	d_2	26 mm
Length of the spring tape	L_s	65 cm
Thickness of the spring tape	t_1	0.2 mm
Width of the spring tape	b_1	12 mm
Moment of the motor	M_m	1.5 Nm
Radius of the output drum	R_m	17.5 mm
Revolutions of the motor	ω_m	15 r/min

positive slope as the deployed boom length increases, which means the energy requirement is satisfied and the system can function correctly [10].

5. FEM simulation

To validate the design results above, the FEM will be carried out to analyse the lenticular boom. Using a static analysis, we will calculate the bending, torsional, flattening and wrapping stress of the lenticular boom; while using a dynamic analysis, we will analyse the natural frequency and the energy in the flattening/wrapping process of the lenticular boom.

5.1. Static analysis

Using a bending and torsional analysis, a three-dimensional FEM model of the lenticular boom with a tip plate is built using the software Ansys. The tip plate is added to the end of the boom to prevent distortion of the section at the tip during its bending or torsion. The boom is modelled using an isotropic shell material and discretised into 4000 elements with a solid-shell. The tip plate is treated as rigid and with a mass of 0.7 kg. We set the contact between the boom end and the tip plate as bonded (always) to insure a compact contact. During bending analysis, the boom with the tip plate is subjected to a 1 g acceleration. While in torsional analysis, a torsional moment of 1 Nm is applied to the tip plate, and the simulation type is a small-deformation static analysis. The bending result along the x-axis and the torsional result of the boom are shown in Fig. 9. The numerical results are listed in Table 4, and these results are almost the same as the theoretical predictions.

For a flattening analysis, the boom with two rigid flat plates is shown in Fig. 10(a). Here, to save simulation time, half of the boom shell with a length of 2 cm is analysed. The boom is modelled using an isotropic shell material and discretised into 1000 elements with shell 164. The two rigid flat plates are modelled as RIGI material with solid. All the degrees of freedom of the rigid plates except the y-axis translation are constrained. The two contact types are selected to be ASTS type, and the simulation type is a large-deformation static analysis. When flattening the boom, the upper rigid plate moves down slowly and lays flat against the boom. The stress results are shown in Fig. 10(a) and Table 4. The stress in the neutral surface of the boom is also shown in Fig. 10(b). In essence, the results are close to the theoretical predictions except for some big deviations ($x = 3.6, 8.6$) and small

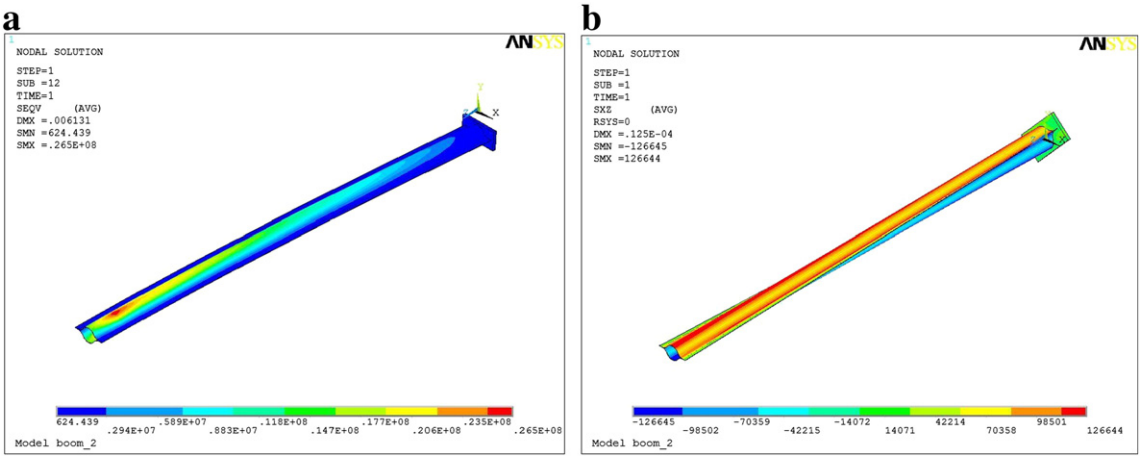

Fig. 9. (a) FEM bending analysis of the lenticular boom. (b) FEM torsional analysis of the lenticular boom.

Table 4
Static analysis results of the lenticular boom.

Parameter	Theory	FEM
Maximum bending stress along the *x*-axis	25.02 MPa	26.5 MPa
Maximum bending stress along the *y*-axis	11.88 MPa	12.4 MPa
Maximum torsional stress	0.1203 MPa	0.1267 MPa
Maximum flattening stress along the *x*-axis	573 MPa	513 MPa
Maximum wrapping stress along the *y*-axis	612 MPa	648 MPa

fluctuations. The big deviations are physically existed because the undistorted point D decreases the stress (see Fig. 3), while a constant stress is supposed in theoretical prediction (Eq. (11)). The small fluctuations are probably caused by the uneven flatting of the boom against the rigid flat plates and numerical errors in the finite element simulation.

In the wrapping analysis, a rigid storage reel with a boom wrapped on the reel is modelled. To save simulation time, half of the boom shell with a length of 30 cm is analysed. The definitions of the materials, elements, contacts and the simulation type are similar to those of the flattening process. When wrapping the boom, the rigid storage reel rotates along its central axis and wraps the boom. The stress results are shown in Fig. 11(a) and Table 4. The stress in the neutral surface of the boom is drawn in Fig. 11(b) and is nearly uniform around the storage reel. The result of small fluctuations is similar to that of a flattening analysis.

5.2. Dynamic analysis

5.2.1. Natural frequency

The elements, material and conditions used in the simulation are similar to the parameters used in the bending/torsional analyses to obtain the natural frequency of the deployable boom [23]. The numerical results are shown in Fig. 12 and are listed in Table 5. From these results, we can see that the FEM results are identical to the theoretical predictions.

5.2.2. Energy calculation

As mentioned above, the energy equilibrium of the system is very important. The theoretical relationship between the strain energy and the deployed boom length has been addressed in Fig. 8(b). Here, we simply calculate the energy of the boom during the flattening and wrapping processes. Models have been built that are similar to those used in the static analysis (Figs. 10(a), 11(a)). During the calculation of the flattening and the wrapping energy, we create a plot of the flattening and the wrapping energy versus the displacement of the upper rigid plate and compare the result with theoretical prediction (as shown in Fig. 13(a) and (b), respectively). The numerical results of both flattening and wrapping are listed in Table 5. The energy in the theoretical prediction is simply treated as a perfect linear relationship with the displacement/angle, so there is a slight difference between the results of the FEM and the theoretical prediction especially with respect to the displacement of the rigid plate and the angle of the storage reel increasing. However, the FEM and the theoretical results have a consistent trend and identical results.

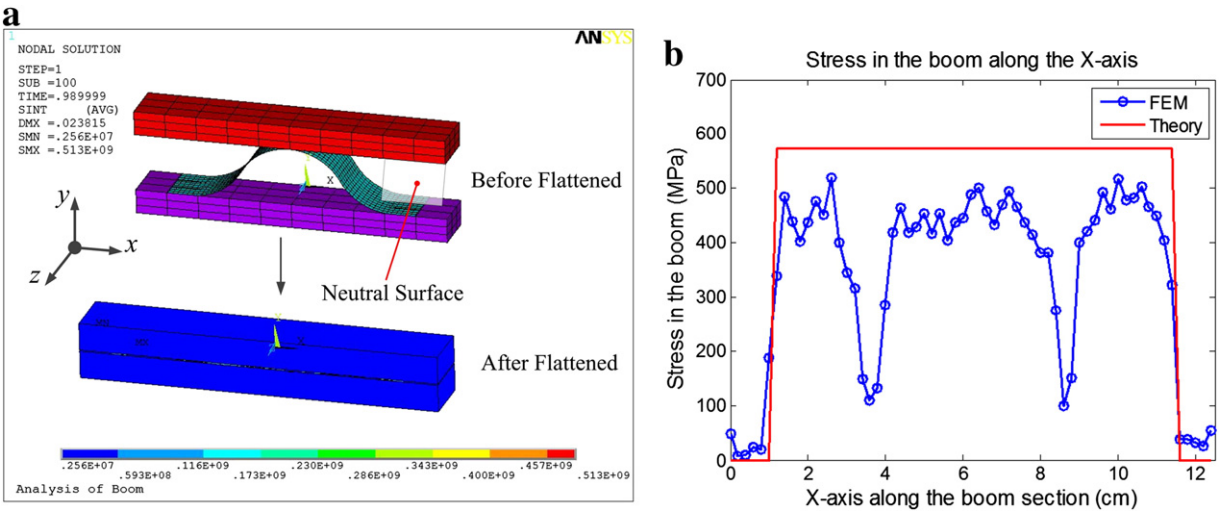

Fig. 10. (a) FEM flattening analysis of the lenticular boom. (b) Stress in the neutral surface of the boom when flattened.

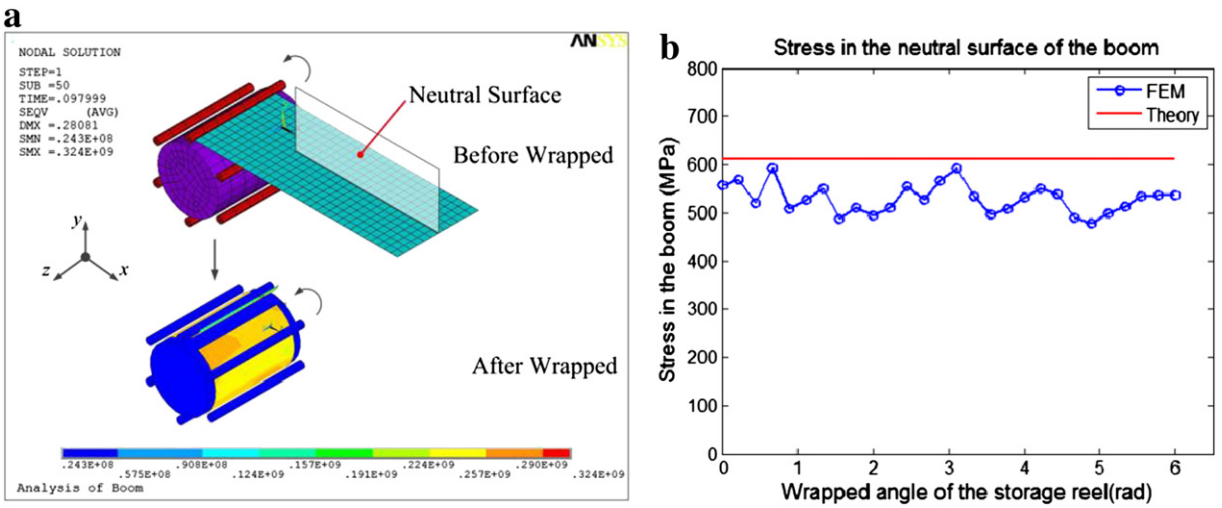

Fig. 11. (a) FEM wrapping analysis of the lenticular boom. (b) Stress in the neutral surface of the boom when wrapped.

6. Conclusion

This paper presents the design theory and dynamic analysis of a deployable boom for use in small spacecraft to hold a space probe away from the spacecraft body. The proposed deployable boom is composed of a lenticular boom with a storage reel, a retractable/deployable mechanism and other auxiliary devices. Specifically, considering the involved geometrical limitations and

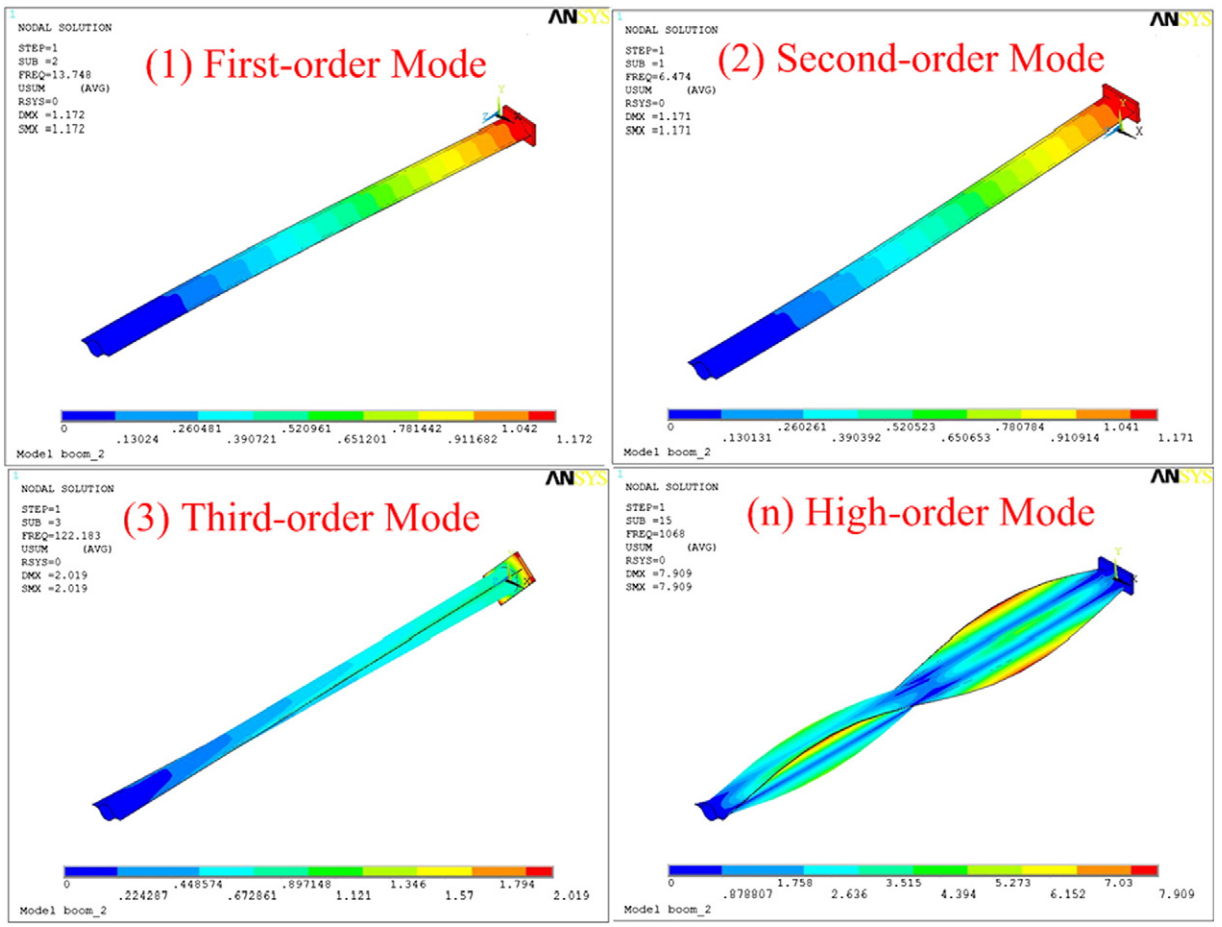

Fig. 12. FEM modal analysis of the lenticular boom.

Table 5
Dynamic analysis results of the lenticular boom.

Parameter	Theory	FEM
First-order frequency of the boom	6.5770 Hz	6.4736 Hz
Second-order frequency of the boom	13.8992 Hz	13.748 Hz
Total energy in flattening process	0.2617 J	0.3530 J
Total energy in wrapping process	1.17 J	1.38 J

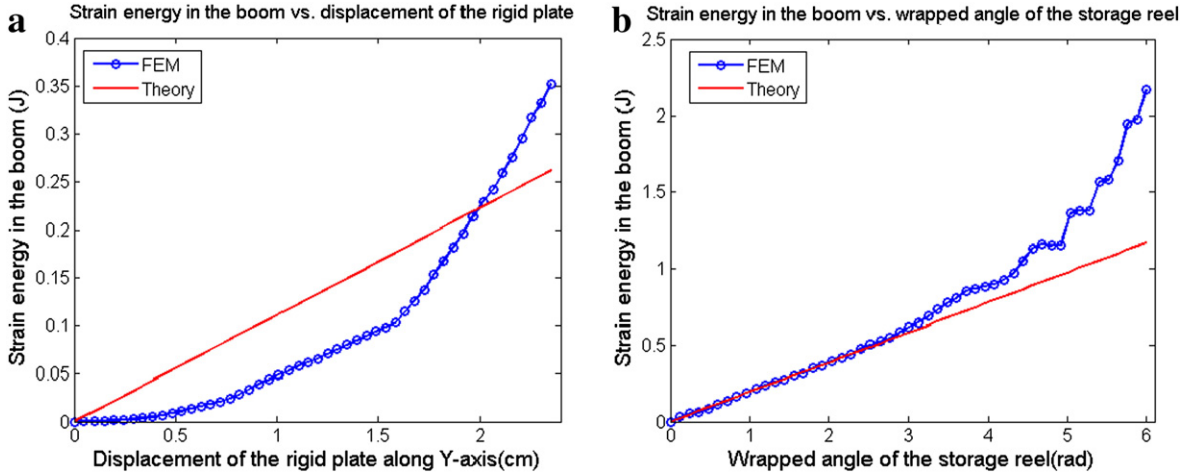

Fig. 13. (a) FEM energy analysis in flattening process. (b) FEM energy analysis in wrapping process.

physical constraints, the optimal design of the lenticular boom with the storage reel and the retractable/deployable mechanism are carried out. Here, SQP is adopted to reduce the computational complexity of the optimisation. Then, the preliminary parameters of the deployable boom are specified. Lastly, FEM simulations are developed to investigate the mechanical behaviours of the lenticular boom. The results validate the efficiency of the design.

The next step is to implement experimental work on a terrestrial deployable boom system, which has been manufactured in our laboratory, and more work should be performed in both theoretical and further experimental demonstration.

Acknowledgements

This work was jointly supported by the National Natural Science Foundation of China (Grant Nos. 51375034, 50905006) and the Research Fund for the Doctoral Program of Higher Education (Grant No. 20091102120027).

References

[1] S.K. Michael, On-orbit space shuttle inspection system utilizing an extendable boom, Aerospace Engineering, the University of Maryland, 2004. (Master thesis).
[2] D. Auslander, J. Cermenska, G. Dalton, Instrument boom mechanisms on the THEMIS satellites; magnetometer, radial wire, and axial booms, Space Sci. 141 (2008) 185–211.
[3] C. Sickinger, L. Herbeck, T. Ströhlein, J. Torrez-Torres, Lightweight deployable booms: design, manufacture, verification, and smart materials application, Proceeding of the 55th International Astronautical Congress, 2004.
[4] M. Leipold, H. Runge, C. Sickinger, Large sar membrane antennas with lightweight deployable booms, Proceeding of the 28th ESA Antenna Workshop on Space Antenna Systems and Technologies, ESA/ESTEC, May 1–June 3 2005.
[5] C. Sickinger, L. Herbeck, E. Breitbach, Structural engineering on deployable CFRP booms for a solar propelled sailcraft, Acta Astronaut. 58 (2006) 185–196.
[6] J.M. Fernandeza, V.J. Lappas, A.J. Daton-Lovett, Completely stripped solar sail concept using bi-stable reeled composite booms, Acta Astronaut. 69 (2010) 78–85.
[7] J. Block, M. Straubel, M. Wiedemann, Ultralight deployable booms for solar sails and other large gossamer structures in space, Acta Astronaut. 68 (2010) 984–992.
[8] F.A. Roybal, J.A. Banik, T.W. Murphey, Development of an elastically deployable boom for tensioned planar structures, Proceeding of the 48th AIAA/ASME/ASCE/AHS/ASC Structures, Structural Dynamics, and Materials Conference, Honolulu, Hawaii, April 23–26 2007.
[9] G.M. Thomas, Prototype Development and Dynamic Characterization of Deployable Cubesat Booms, Technology Air University, 2010. (Master thesis).
[10] F. Rehnmark, M. Pryor, B. Homes, D. Schaechter, N. Pedreiro, Development of a deployable nonmetallic boom for reconfigurable systems of small spacecraft, Proceeding of the 48th AIAA/ASME/ASCE/AHS/ASC Structural Dynamics & Materials Conference, Honolulu, Hawaii, April 23–26 2006.
[11] F. Hakkak, S. Khoddam, On calculation of preliminary design parameters for lenticular booms, Aerosp. Eng. 221 (2006) 377–384.
[12] S.D. Guest, S. Pellegrino, Analytical models for bistable cylindrical shells, R. Soc. 462 (2006) 839–854.

[13] E. Kebadze, S.D. Guest, S. Pellegrino, Bistable prestressed shell structures, Int. J. Solids Struct. 41 (2004) 2801–2820.
[14] K.A. Seffen, Z. You, S. Pellegrino, Folding and deployment of curved tape springs, Int. J. Mech. Sci. 42 (2000) 2055–2073.
[15] E.A. Lemaster, D.B. Schaechter, C.K. Carrington, Experimental demonstration of technologies for autonomous on-orbit robotic assembly, Proceeding of the Space 2006, San Jose, California, September 19–21 2006.
[16] R.X. Li, W.J. Chen, G.Y. Fu, J.Z. Zhao, Numerical simulation of flattening and wrapping process of lenticular wrapped-rib, J. Acta Astronaut. 32 (1) (2011) 224–231(in Chinese).
[17] R.X. Li, W.J. Chen, G.Y. Fu, Experimental and stowing/deploying dynamical dimulation of lenticular carbon fiber reinforced polymer thin-walled tubular space boom, J. Shanghai Jiaotong Univ. (Sci.) 17 (1) (2012) 58–64.
[18] R. Yao, X. Tang, J. Wang, P. Huang, Dimensional optimization design of the four-cable-driven parallel manipulator in FAST, IEEE/ACM Trans. Mechatron. 15 (6) (2010) 932–941.
[19] H.Z. Jiang, Z.Z. Tong, J.F. He, Dynamic isotropic design of a class of Gough–Stewart parallel manipulators lying on a circular hyperboloid of one sheet, Mech. Mach. Theory 46 (2011) 358–374.
[20] W.C. Young, R.G. Budynas, Roark's Formulas for Stress and Stress, McGraw-Hill Companies Inc, New York, 2002.
[21] V. Sangwan, S.K. Agrawal, Differentially flat design of bipeds esuring limit cycles, IEEE/ACM Trans. Mechatron. 14 (6) (2009) 647–657.
[22] Optimization Toolbox User's Guide, Mathwork Inc., 2010
[23] G. Aridon, L. Blanchard, A. Allezy, On the correction capability of a deployed tape-spring hexapod, Mech. Mach. Theory 43 (2008) 1009–1023.

ZhongYi Chu was born in Hebei Province, China in 1977. He received a Ph.D. degree from the Robotics Research Institute, Harbin Institute of Technology, Harbin, China, in 2004. In 2006, he was a postdoctoral fellow in the State Key Laboratory of Intelligent Technology and Systems, Tsinghua University, Beijing, China. Currently, he is an associate professor with the School of Instrument Science and Opto-electronics, Beihang University, Beijing, China. His research interests include advanced robotics and control.